Cell Metabolism
Short Article

Local Proliferation of Macrophages Contributes to Obesity-Associated Adipose Tissue Inflammation

Shinya U. Amano,[1,2] Jessica L. Cohen,[1,2] Pranitha Vangala,[1] Michaela Tencerova,[1] Sarah M. Nicoloro,[1] Joseph C. Yawe,[1] Yuefei Shen,[1] Michael P. Czech,[1,*] and Myriam Aouadi[1,*]
[1]Program in Molecular Medicine, University of Massachusetts Medical School, Worcester, MA 01605, USA
[2]These authors contributed equally to this work
*Correspondence: michael.czech@umassmed.edu (M.P.C.), myriam.aouadi@umassmed.edu (M.A.)
http://dx.doi.org/10.1016/j.cmet.2013.11.017

SUMMARY

Adipose tissue (AT) of obese mice and humans accumulates immune cells, which secrete cytokines that can promote insulin resistance. AT macrophages (ATMs) are thought to originate from bone-marrow-derived monocytes, which infiltrate the tissue from the circulation. Here, we show that a major fraction of macrophages unexpectedly undergo cell division locally within AT, as detected by Ki67 expression and 5-ethynyl-2′-deoxyuridine incorporation. Macrophages within the visceral AT (VAT), but not those in other tissues (including liver and spleen), displayed increased proliferation in obesity. Importantly, depletion of blood monocytes had no impact on ATM content, whereas their proliferation in situ continued. Treatment with monocyte chemotactic protein 1 (MCP-1) induced macrophage cell division in AT explants, whereas *mcp-1* deficiency in vivo decreased ATM proliferation. These results reveal that, in addition to blood monocyte recruitment, in situ proliferation driven by MCP-1 is an important process by which macrophages accumulate in the VAT in obesity.

INTRODUCTION

Obesity can induce an insulin-resistant state in adipose tissue (AT), liver, and skeletal muscle and is a strong risk factor for the development of type 2 diabetes (Guilherme et al., 2008; Olefsky and Glass, 2010). It is increasingly appreciated that the accumulation of macrophages and other immune cell types in AT correlates with a chronic inflammatory state that ultimately impairs adipocyte function and may contribute to the development of insulin resistance (Aouadi et al., 2013;Olefsky and Glass, 2010; Weisberg et al., 2003).

The origin of macrophages in AT has previously been attributed to the recruitment of blood monocytes into AT on the basis of one study using irradiation followed by bone marrow transplant (Weisberg et al., 2003). Therefore, strategies to decrease AT macrophage (ATM) accumulation have been particularly focused on decreasing macrophage migration into the AT by depleting blood monocytes or genes encoding chemokines that attract macrophages into the AT (Feng et al., 2011; Kanda et al., 2006; Nomiyama et al., 2007; Weisberg et al., 2006). However, studies using these approaches do not address whether migration is the only process contributing to macrophage accumulation in the AT. The present study was designed to determine whether significant macrophage cell division also occurs within visceral AT (VAT) in mice.

RESULTS AND DISCUSSION

Macrophages Proliferate Locally within the Adipose Tissue

To confirm macrophage accumulation in AT of obese mice, we used 8- to 12-week-old genetically obese (*ob/ob*) male mice and their lean control wild-type (WT) littermates. The stromal-vascular fraction (SVF) from VAT and subcutaneous AT (SAT) was stained with antibodies against macrophage markers, F4/80 and CD11b, an eosinophil marker, Siglec-F, and a neutrophil marker, Gr-1, and analyzed with flow cytometry. The macrophage population in the AT was defined as $F4/80^{+}/CD11b^{+}/Siglec\text{-}F^{-}/Gr\text{-}1^{-}$ (for the complete gating scheme, see Figure S1A available online). Consistent with published studies (Weisberg et al., 2003; Xu et al., 2003), macrophage content was significantly increased in the VAT of *ob/ob* in comparison to WT mice (*ob/ob* $959 \pm 69 \times 10^3$ versus WT $140 \pm 35 \times 10^3$ macrophages per g of VAT, $p < 0.001$; Figures 1A and 1B). The number as well as the percentage of macrophages was also increased in the SAT of *ob/ob* in comparison to WT mice but to a lower extent than in VAT (*ob/ob* $192 \pm 31 \times 10^3$ versus WT $109 \pm 12 \times 10^3$ macrophages per g of SAT, $p = 0.04$; Figure S1B). These results confirmed that macrophages accumulate mostly in the VAT in mice in response to obesity.

To test whether ATM proliferation increases in the inflammatory setting of obesity, SVF cells from WT and *ob/ob* mice were stained with an antibody against the proliferation marker Ki67, which is a protein expressed during all active phases of the cell cycle (Scholzen and Gerdes, 2000). Ki67 signal was detected in approximately 2.3% of ATMs from VAT of lean WT mice and in 10% of ATMs of *ob/ob* mice (*ob/ob* $94 \pm 7 \times 10^3$ versus WT $7.6 \pm 3.2 \times 10^3$ macrophages per g of VAT, $p < 0.001$; Figures 1C and 1D). The percentage of $Ki67^{+}$ macrophages was also increased in the SAT from *ob/ob* in comparison to WT mice (Figure S1C). However, the number of $Ki67^{+}$ macrophages was lower in SAT in comparison to VAT in *ob/ob* mice (SAT $20.0 \pm 3.3 \times 10^3$ versus VAT $94 \pm 7 \times 10^3$ macrophages per g, $p < 0.001$). This suggests that macrophages preferentially

accumulate and proliferate in the VAT of obese mice. Consistent with the flow cytometry analysis, immunofluorescence microscopy on SVF cells and VAT of *ob/ob* mice showed macrophages expressing Ki67 in their nuclei (Figures 1E and 1F). Interestingly, most of the Ki67 staining was observed in macrophages in a region of the VAT rich in macrophages termed crown-like structures (CLSs) (Figure 1F).

Similar to genetically induced obesity, diet-induced obesity increased macrophage content in the AT (Figures 1G and 1H). ATM number was significantly higher in SVF of VAT in mice fed a high-fat diet (HFD) in comparison to normal chow diet (ND) (HFD $1,045 \pm 131 \times 10^3$ versus ND $140 \pm 35 \times 10^3$ macrophages per g of VAT, $p < 0.001$). More importantly, in mice fed an HFD, 17% of ATMs were $Ki67^+$ in comparison to 3% in mice fed an ND (HFD $183 \pm 21 \times 10^3$ versus ND $7.6 \pm 3.2 \times 10^3$ macrophages per g of VAT, $p < 0.001$; Figures 1 I and 1J). Consistent with published data (Bourlier et al., 2008), and as suggested by gene expression profile analysis of human ATMs (Mayi et al., 2012), flow cytometry analysis of SVF stained with Ki67 antibody showed that approximately 8% of ATMs proliferate in AT (7.7% ± 1.9%, n = 5; Figure 1K). Altogether, with the use of flow cytometry and microscopic analysis, these results show that macrophages express the proliferation marker Ki67 in the AT in mice and humans and, to a higher degree, in response to obesity caused by either genetic manipulation or an HFD in mice.

Next, we tested whether fasting-induced weight loss also regulates ATM proliferation. After a 24 hr fast, mice lost an average of 5 percent body weight (data not shown). Although the percentage of ATM was slightly decreased, the number of ATM was significantly decreased in VAT of mice fed an HFD after a 24 hr fast (Figures 1L and 1M). Although this could be explained by a concomitant decrease in nonmacrophage cells, it has been shown that fasting induces the formation of lipid-laden macrophages attached to the adipocyte fraction (Kosteli et al., 2010). Interestingly, ATM proliferation was significantly decreased after a 24 hr fast, suggesting a correlation between macrophage content and proliferation in the AT (Figure 1N).

It is interesting to note that fasting had no effect on the proliferation of $F4/80^-/CD11b^-$ cells, which could include cell types that have been shown to proliferate in situ in the AT, including T cells (Morris et al., 2013a) and adipocyte progenitors (Lee et al., 2012) (Figure 1O). Altogether, these results suggest that changes occurring during AT mass regulation selectively affect proliferation of specific cell types in AT, including macrophages.

Obesity Stimulates Macrophage Proliferation Specifically in the Adipose Tissue

To test whether macrophage proliferation increases with obesity in tissues other than AT, we analyzed the proliferation rate of macrophages in the spleen and liver after a 3 hr pulse of the nucleoside analog to thymidine, 5-ethynyl-2′-deoxyuridine (EdU), which is incorporated into DNA only during the S phase. Approximately 1% of ATMs in lean mice and about 4.5% of the macrophages in the obese mice were in S phase during the pulse of EdU (Figure 2A), confirming that obesity increases ATM proliferation. In contrast, less than 2% of all cells, including macrophages, were EdU^+ in spleen and liver, and there was no difference in EdU^+ cells between lean and obese mice in these tissues (Figures 2B and 2C). This striking specificity for increased macrophage proliferation in AT in obesity implies that the AT microenvironment is important for macrophage proliferation.

Monocytes failed to display detectable EdU incorporation within the 3 hr pulse in lean or obese mice, suggesting that EdU^+ macrophages observed in the AT are not recently recruited blood monocytes (Figure 2D). Importantly, obesity did not affect the EdU incorporation rate in spleen, liver, or blood macrophages (Figure 2E). Interestingly, macrophage content increased with obesity in AT (Figure 1A), whereas there was no change or a slight decrease in spleen or liver in *ob/ob* mice in comparison to WT mice (Figure 2F). Furthermore, this confirms a correlation between macrophage accumulation and proliferation in tissues and suggests that AT provides a unique environment facilitating macrophage proliferation.

In order to study the selective effect of obesity on immune cell proliferation, we analyzed Ki67 staining in eosinophils and neutrophils, whose content in the AT has been shown to be regulated by obesity (Talukdar et al., 2012; Wu et al., 2011). Consistent with a prior report (Wu et al., 2011), we found that eosinophil content relative to macrophages in the AT decreased with obesity (Figures S2A–S2C). Neutrophil content in AT was not significantly different between WT and *ob/ob* mice (Figures S2D–S2F). Although both eosinophils and neutrophils have been shown to have some proliferative capacity outside of the bone marrow (Bjornson et al., 1985; Yang and Renzi, 1993), we failed to detect any EdU incorporation into these cells within AT (Figures S2C and S2F). Our results suggest that obesity does not stimulate the proliferation of all cells in the AT but selectively stimulates the proliferation of specific cell types, including macrophages.

Macrophage Proliferation Contributes to Adipose Tissue Inflammation Independently of Monocyte Recruitment

Next, to further ensure that the proliferating macrophages in the AT were not recently recruited EdU^+ blood monocytes, we studied the capacity of ATMs to proliferate ex vivo. SVF cells isolated from VAT of lean and obese mice were plated and treated with EdU for 3 hr. Approximately 0.3% of the ATMs from lean mice were EdU^+, whereas >2% were positive in macrophages from obese mice (Figures S3A and S3B). These results suggest that ATMs have the inherent capacity to proliferate ex vivo independently of blood monocyte recruitment. To test this hypothesis, we depleted blood monocytes in *ob/ob* mice by intravenous (i.v.) injection of clodronate-loaded liposomes (Clod-Lipo), which induce apoptosis once ingested by monocytes (Feng et al., 2011). Consistent with published studies, Clod-Lipo i.v. injection depleted about 80% of blood monocytes 16 hr after injection in comparison to a PBS-liposome (PBS-Lipo) injection (Figures 3A and 3B). Then, we injected *ob/ob* mice every 16 hr with Clod-Lipo in order to maintain blood monocyte depletion and measured macrophage content in the VAT. Unexpectedly, ATM absolute number (48 hr, PBS-Lipo 3.78 ± 0.37 versus Clod-Lipo 3.88 ± 0.35; 96 hr, PBS-Lipo 4.54 ± 0.60 versus Clod-Lipo 3.36 ± 0.11 $\times 10^6$ cells per g of VAT) and ATM percentage in the SVF were unchanged with Clod-Lipo treatment even after prolonged blood monocyte depletion (Figure 3C). These data raised the possibility that the increase in macrophages that occurs during obesity was largely the result of the

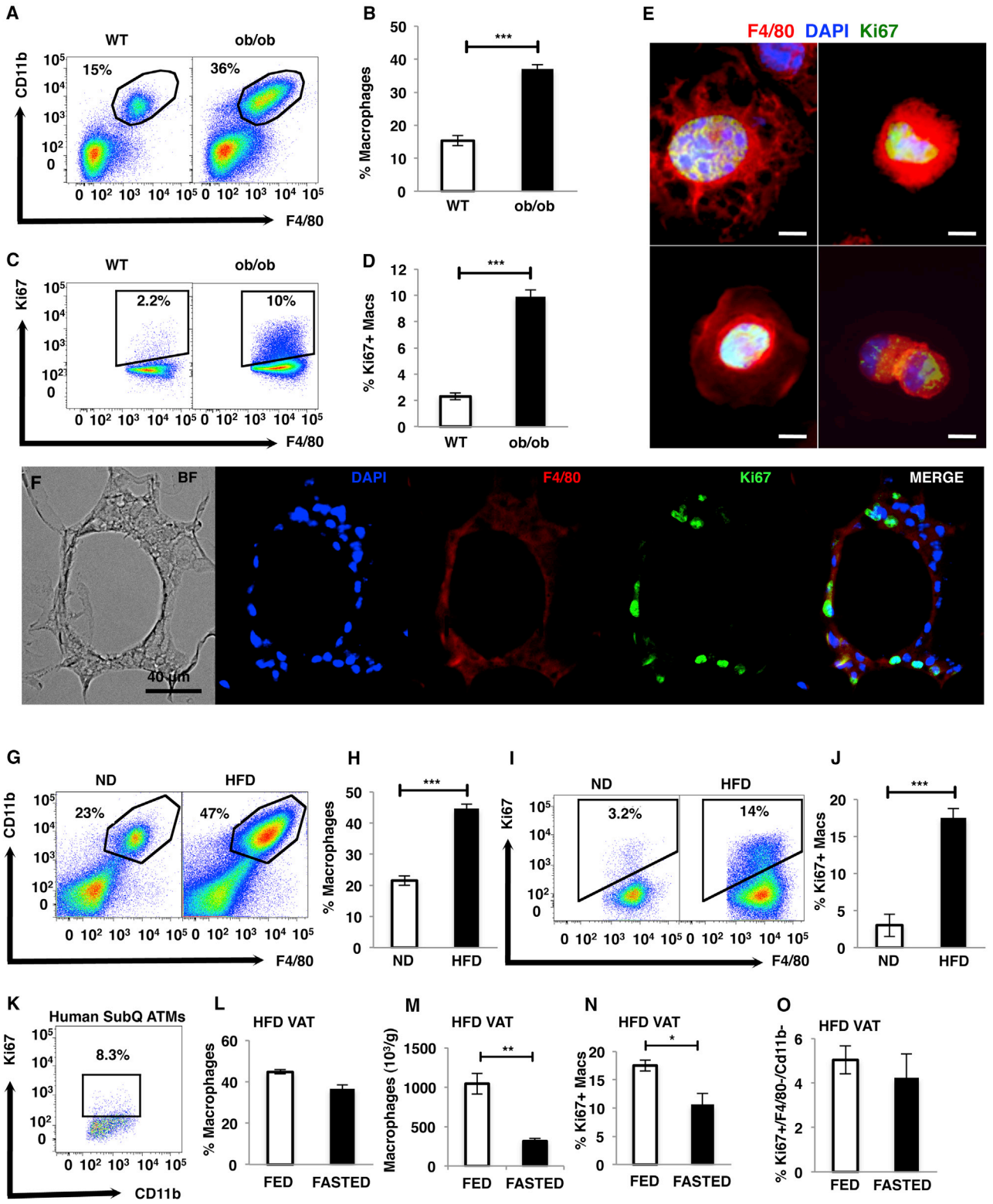

Figure 1. Adipose Tissue Macrophages Express the Cell Division Marker Ki67

SVF from VAT of WT and ob/ob mice was isolated and analyzed by flow cytometry.

(A) Representative flow cytometry dot plots.

(B) Percentage of macrophages in SVF.

(C) Representative flow cytometry dot plots of ATMs stained with Ki67.

(legend continued on next page)

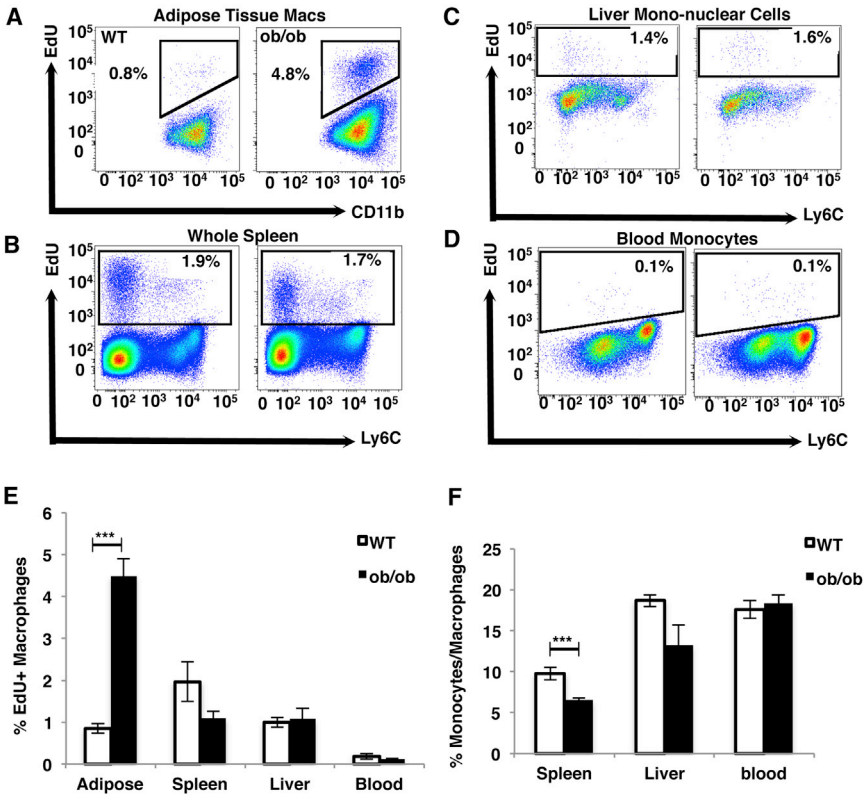

Figure 2. Obesity Increases Macrophage Proliferation Specifically in Adipose Tissue

(A–D) WT and *ob/ob* mice were intraperitoneal injected with EdU, and AT (A), spleen (B), liver (C), and blood (D) were collected and digested 3 hr after treatment. All cells were stained and analyzed by flow cytometry. Representative dot plots depict the EdU incorporation into all cells of the respective tissues or blood monocytes.

(E) Mean percentage of EdU incorporation rate of the macrophages of each tissue ± SEM.

(F) Percentage of macrophages in each tissue. n = 14–15 from three independent experiments for AT and blood, and n = 9–10 from two independent experiments for spleen and liver. Statistical significance was determined by a Student's t test. ***$p < 0.001$.

See also Figure S2.

proliferation of the resident population. Therefore, *ob/ob* mice were given EdU in drinking water during monocyte depletion, as depicted in the diagram in Figure 3D. About half of the macrophages in the AT of *ob/ob* mice injected with PBS-Lipo had incorporated EdU 80 hr after EdU exposure (Figures 3E and 3F). Importantly, the depletion of blood monocytes had no effect on macrophage proliferation, as observed by the EdU incorporation in the VAT of *ob/ob* mice injected with Clod-Lipo (Figures 3E and 3F). Interestingly, no difference in EdU incorporation was observed in macrophages in SAT of *ob/ob* in comparison to WT mice after 80 hr of EdU exposure (Figure 3G). This suggested that macrophage proliferation plays a major role in VAT macrophage expansion in obesity independently of monocyte recruitment. However, recently recruited macrophages may also proliferate in AT of obese mice, given that a recent study showed that 5% of labeled blood monocytes transferred from donor into recipient mice express Ki67 in the host AT 2 days after transfer (Oh et al., 2012).

Although macrophage subpopulations in the AT may have overlapping marker expression profiles, it is generally thought that CD11c expression is characteristic of proinflammatory macrophage subtypes (Lumeng et al., 2008). Therefore, we analyzed the rate of proliferation of proinflammatory ($CD11c^+$) and anti-inflammatory ($CD11c^-$) macrophages (Figure S3C). We failed to observe any difference in the rate of proliferation of macrophage population subtypes. This suggests that obesity increases macrophage proliferation rate independently of their inflammatory state. It has been previously shown that CLS density is higher in the VAT in comparison to SAT in obese mice (Murano et al., 2008). Interestingly, microscopic analysis of VAT sections showed that EdU was mostly incorporated in macrophages in CLS (Figure 3H). Altogether, these results suggest that ATM proliferation occurs at a high rate in the VAT, where macrophage content and CLS density are greatly increased by obesity.

(D) Percentage of macrophages expressing Ki67. n = 30–31 from six independent experiments.

(E) Microscopy of plated SVF stained with antibodies against F4/80 (red) and Ki67 (green). Nuclei were stained with DAPI (blue). 63× magnification images. The scale bar represents 5 μm.

(F) VAT of *ob/ob* mice containing CLS stained with antibodies against F4/80 (red) and Ki67 (green). Nuclei were stained with DAPI (blue). 20× magnification images. The scale bar represents 40 μm.

(G) SVF from VAT of mice fed an ND or HFD for 7 weeks was isolated and analyzed by flow cytometry. Representative flow cytometry dot plots.

(H) Mean percentage of macrophages in SVF.

(I) Representative flow cytometry dot plots of ATMs stained with Ki67.

(J) Percentage of macrophages expressing Ki67. n = 30–31 from six independent experiments.

(K) Representative dot plot of SVF from human SAT stained with Ki67.

(L) Percentage of macrophages in SVF from VAT of mice fed an HFD for 7 weeks and fasted for 24 hr. n = 8–18.

(M) Number of macrophages in SVF from VAT of mice fed an HFD and fasted for 24 hr. n = 5.

(N) Percentage of macrophages expressing Ki67 in fasted mice. n = 8–18.

(O) Percentage of nonmacrophages ($CD11b^-/F4/80^-$) expressing Ki67. n = 8–18. All graphs are expressed as mean ± SEM. Statistical significance was determined by a Student's t test. ***$p < 0.001$; **$p < 0.01$; *$p < 0.05$.

See also Figure S1.

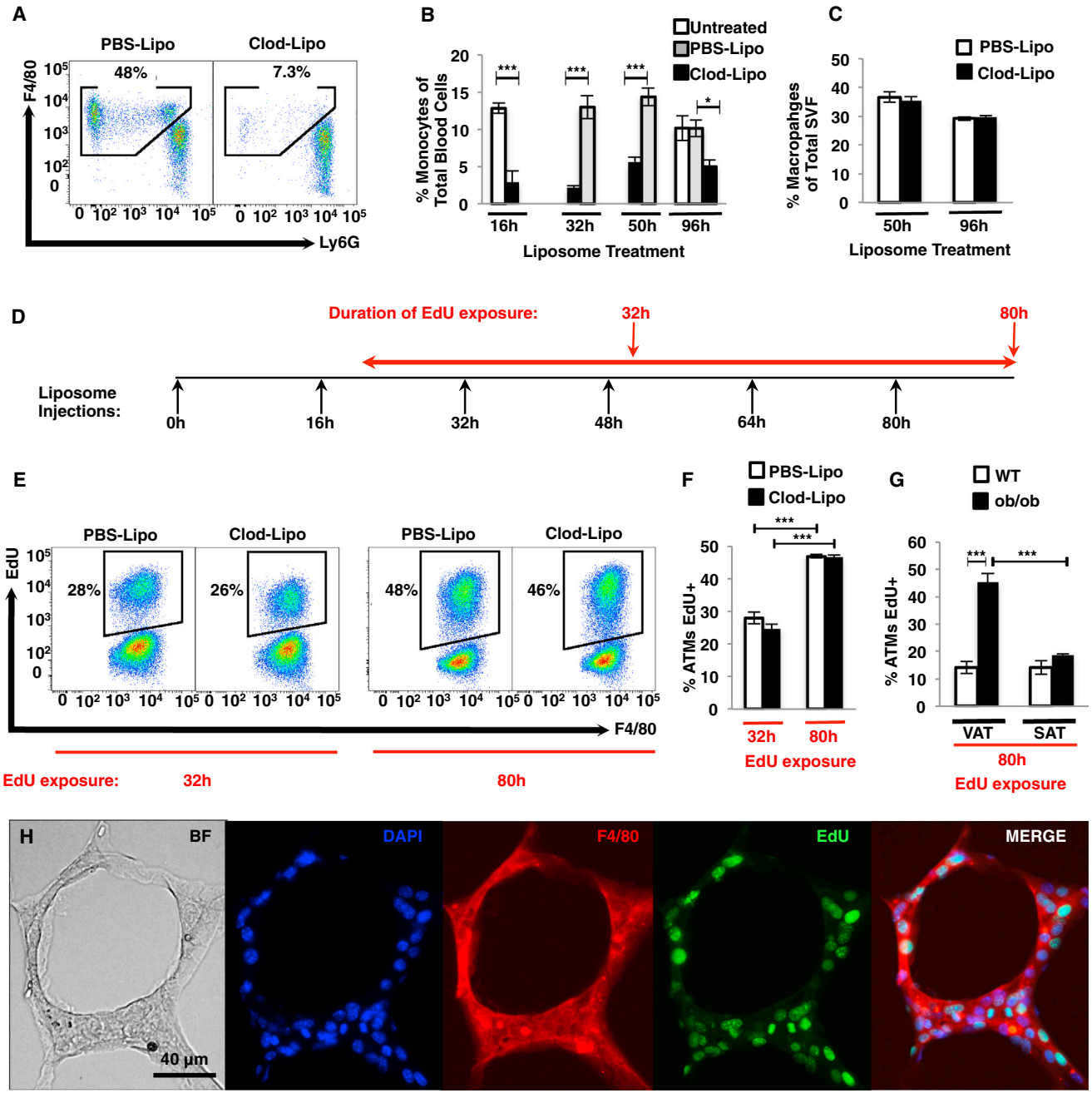

Figure 3. Adipose Tissue Macrophages Proliferate Independently of Monocyte Recruitment

(A and B) Example flow cytometry dot plots of $CD11b^{+}$ blood cells show the depletion of monocytes.

(B) The quantitation of blood monocytes expressed as a percentage of total blood cells. n = 10 for 16–48 hr of liposome treatment, and n = 4–5 for the 96 hr time point.

(C) Macrophage content in the AT of PBS-Lipo- and Clod-Lipo-treated *ob/ob* mice. n = 5 mice per group. 18 hr after initial injection, the mice were given drinking water containing EdU.

(D) Diagram representing the experimental design of the treatment.

(E and F) Representative flow cytograms (E) and quantificationn (F) of EdU incorporation into ATMs during 32 and 80 hr of exposure to EdU drinking water in PBS-Lipo-treated and monocyte-depleted Clod-Lipo-treated *ob/ob* mice.

(G) Quantification of EdU incorporation into ATMs during 80 hr of exposure to EdU drinking water in VAT and SAT in lean WT and *ob/ob* obese mice. n = 5 mice per group. All graphs are expressed as mean ± SEM. Statistical significance was determined by a Student's t test or two-way ANOVA followed by a Tukey post hoc test. ***$p < 0.001$; **$p < 0.01$; *$p < 0.05$.

(H) VAT of *ob/ob* mice containing CLS stained with antibodies against F4/80 (red) and EdU (green). Nuclei were stained with DAPI (blue). 20× magnification images. The scale bar represents 40 µm.

ob/ob mice were i.v. injected with either PBS-Lipo or Clod-Lipo every 16 hr. See also Figure S3.

MCP-1 Stimulates Adipose Tissue Macrophage Proliferation

To investigate the mechanism by which obesity stimulates macrophage proliferation selectively in the AT, we measured the expression of multiple cytokines known to play a role in macrophage proliferation and infiltration in the AT and liver of lean (ND and WT) and obese (HFD and *ob/ob*) mice. These included interleukin 4 (IL-4) (Jenkins et al., 2011), macrophage colony-stimulating factor (M-CSF) (Hashimoto et al., 2013), osteopontin (OPN) (Nomiyama et al., 2007), and monocyte chemotactic protein (also referred to as chemokine [C-C motif] ligand 2 [CCL2/MCP-1]) (Kanda et al., 2006; Weisberg et al., 2006) (Figures 4A–4D and S4A–S4D). Only *opn* and MCP-1 expression were significantly increased with obesity (Figures 4A–4D and S4A–S4D). As described in Figures 1 and 2, macrophage proliferation was mainly increased in VAT in obese mice compared to lean mice; therefore, we measured the expression of *opn* and *mcp-1* in this fat depot in comparison to SAT and liver, where ATM proliferation is minimal (Figures 4E and 4F). Although *opn* expression was unchanged in SAT with obesity, it was significantly increased in the liver (Figure 4E). In addition, *opn* expression was similar in liver and VAT in mice fed an HFD (Figure 4E). In contrast, *mcp-1* expression was significantly higher in VAT in comparison to liver and SAT in obese mice (Figure 4F). In addition, MCP-1 was the only cytokine that was decreased with fasting, which was consistent with a recent study (Asterholm et al., 2012) (Figures 4G and S4E). This suggests a positive correlation between *mcp-1* expression and macrophage proliferation in mice.

On the basis of the above analysis, the expression of *mcp-1* in adipocytes and SVF from VAT of mice fed an HFD was measured. Although *mcp-1* expression was high in both fractions, it was significantly higher in the adipocytes (Figure S4F). Interestingly the MCP-1 receptor, chemokine (C-C motif) receptor 2 (CCR2), has been shown to be mostly expressed in macrophages in CLS where most of proliferating ATMs were observed (Lumeng et al., 2008). These results suggest that MCP-1 released by adipocytes in CLS could stimulate the proliferation of surrounding ATMs.

In order to test whether MCP-1 regulates ATM proliferation, mice lacking the *mcp-1* gene and their WT littermates were fed an HFD and ATM content, and proliferation was measured in the VAT after 30 hr of EdU administration in drinking water (Figures 4H–4K). HFD-induced obesity significantly increased ATM content, whereas fasting decreased the percentage of macrophages in the VAT (Figures 4H and 4I). Most importantly, we observed a significant decrease in the percentage and number of macrophages in the VAT from MCP-1 knockout (KO) in comparison to WT (Figures 4H and 4I). RT-PCR analysis revealed that *emr1* and *cd11b* expression was decreased in the VAT of MCP-1 KO in comparison to WT mice fed an HFD, confirming the decreased ATM content (Figure S4G). In addition, *mcp-1* deficiency was associated with a decrease in the total number of SVF cells (WT-HFD, 1,836.78 ± 256.77 versus MCP-1 KO, 287.96 ± 74.40), suggesting a general effect of MCP-1 on immune cell accumulation in AT, as suggested in other tissues (Allavena et al., 1994; Jimenez et al., 2010). On the other hand, macrophages in the adipose tissue have been shown to play the role of antigen-presenting cells able to induce T cell proliferation (Morris et al., 2013b), suggesting that the decreased ATM accumulation observed in MCP-1 KO mice could result in decreased T cell proliferation. Interestingly, fasting had no additional effect on ATM content in MCP-1 KO, suggesting that MCP-1 could be a major regulator of macrophage content in the VAT (Figures 4H and 4I). EdU staining analysis showed that the percentage and number of EdU^+ ATMs decreases with fasting and *mcp-1* deficiency, suggesting that the decrease in ATM content observed in MCP-1 KO mice could be due to a decreased rate of proliferation (Figures 4J and 4K). Interestingly, *mcp-1* deficiency had no effect on the percentage of macrophages in liver and SAT, confirming the selective role of MCP-1 in the regulation of macrophage content in the VAT (Figure S4H).

Although MCP-1 has been shown to stimulate proliferation of multiple cell types (Hinojosa et al., 2011; Sager et al., 2010), it has been extensively described as a chemokine attracting macrophages from the blood to the AT in obese mice (Kanda et al., 2006; Weisberg et al., 2006). Thus, to test whether MCP-1 regulates ATM proliferation independently of macrophage recruitment, the monocyte content in the blood of MCP-1 KO and WT mice was analyzed (Figure 4L). We observed an increase in circulating monocytes in control mice with HFD in comparison to ND (Figure 4L), suggesting that monocyte recruitment contributes to macrophage accumulation in the AT. However, monocyte number in the blood remained the same in fed and fasted states in MCP-1 KO and WT mice, indicating that fasting-associated MCP-1 decrease or MCP-1 deficiency lowers ATM content mostly by decreasing proliferation (Figure 4L). To test this hypothesis, we measured EdU incorporation in ATM in VAT explants from *ob/ob* mice treated with MCP-1. Consistent with the hypothesis that MCP-1 regulates the accumulation of multiple cell types, the treatment of explants with MCP-1 ex vivo increased the total number of SVCs (untreated, 1,961.15 ± 788.00 versus MCP1 [10 ng/ml], 4,404.80 ± 353.66). Importantly, MCP-1 treatment significantly increased the number of ATMs and EdU incorporation (Figures 4M and 4N). Although proliferation may be regulated by multiple factors, MCP-1 plays a major role in regulating macrophage proliferation in the AT of obese mice independently of monocyte recruitment. However, these data do not exclude the contribution of monocyte recruitment and subsequent proliferation in the AT in obesity.

Next, body weight, glucose tolerance, and fasting glycaemia were measured in MCP-1 KO and WT mice fed an HFD in order to assess the metabolic consequences of a decreased ATM proliferation (Figures 4O–4Q). The body weight of MCP-1 KO was slightly, but not significantly, higher than WT mice fed an HFD, and both were significantly higher than WT mice fed an ND (Figure 4O). Surprisingly, although *mcp-1* deficiency led to a lower rate of macrophage proliferation in the AT and consequently a decreased ATM content, glucose intolerance was exacerbated in MCP-1 KO in comparison to WT mice (Figure 4P). Similarly, fasting blood glucose levels were significantly elevated in MCP-1 KO in comparison to WT mice (Figure 4Q). This result corroborated data from a previous study showing that MCP-1 KO mice fed an HFD are more glucose intolerant that their WT littermates (Inouye et al., 2007). However, Inouye et al. (2007) showed that macrophage content is slightly increased in the

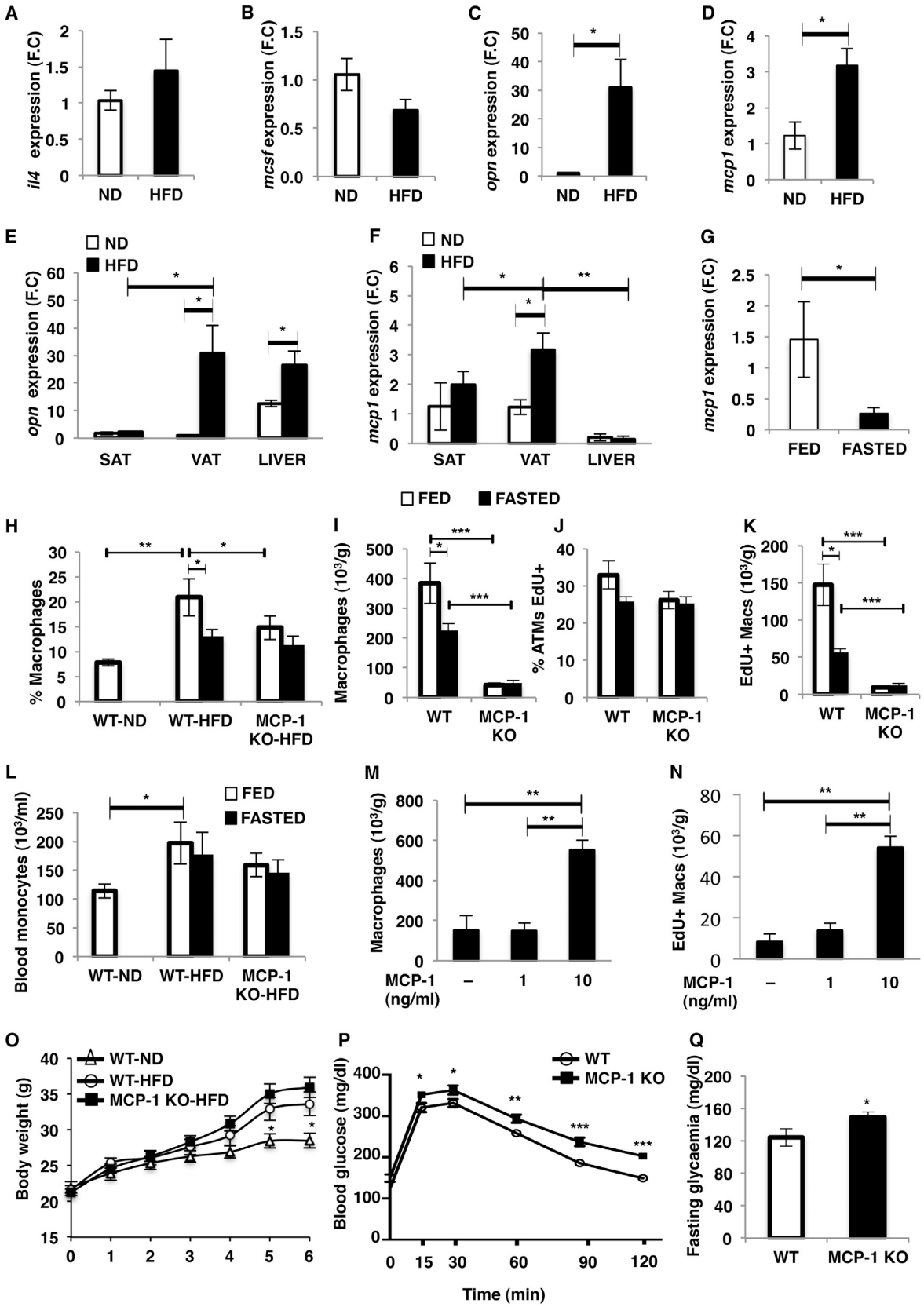

(legend on next page)

VAT of MCP-1 KO in comparison to WT mice. One of the reasons for this discrepancy could be the gating scheme used to define macrophages in the AT. In our study, macrophages were defined as F4/80$^+$/CD11b$^+$/Siglec-F$^-$/Gr1$^-$ (see the gating scheme in Figure S1) versus F4/80$^+$/CD11b$^+$, which includes eosinophils and neutrophils in Inouye et al. (2007).

Altogether, these results show that a decreased ATM proliferation is associated with exacerbated glucose intolerance. Although much of the relevant literature suggests that macrophages in AT are inhibitory to adipose function (Olefsky and Glass, 2010), some data indicate a beneficial role, for example, in increasing adipose lipid storage or clearance of dead cells in AT (Kosteli et al., 2010; Murano et al., 2008). Although MCP-1 deficiency could regulate glucose tolerance independently of an effect on ATM proliferation, such as increased body weight or decreased accumulation of multiple immune cell types, our results indicate that proliferation may be a mechanism mediating the accumulation of ATM beneficial for glucose tolerance.

In summary, we show that macrophage proliferation within VAT is a dynamic mechanism that increases with obesity and decreases during acute weight loss. Given the high proportion of macrophages (about 50%) that incorporate EdU over 80 hr, proliferation most likely contributes significantly, in addition to recruitment, to the accumulation of macrophages in the AT in obesity. At the molecular level, this study reveals MCP-1 as a potential stimulus for macrophage proliferation in obese AT.

EXPERIMENTAL PROCEDURES

Animals

We obtained 8- to 12-week-old male WT C57BL/6J and B6.V-*Lepob*/J (*ob/ob*) mice from Jackson Laboratory and maintained on a 12 hr light/dark cycle. Animals were given free access to food and water. WT C57BL/6J mice were fed an HFD (45% calories from lipids; D12451, Research Diets) for 7 weeks. All other mice were fed normal chow diet (Prolab 5P76 Isopro RMH 3000, LabDiet). We obtained 6-week-old male MCP-1 KO and WT mice on a C57BL/6J background from the Jackson Laboratory. Mice were fed an HFD (60% calories from lipids; D12492, Research Diets) for 6 weeks. All procedures were performed in accordance with protocols approved by the University of Massachusetts Medical School's Institutional Animal Care and Use Committee.

Isolation of Macrophages from Human and Mouse Adipose Tissue

All protocols were approved by the UMass Institutional Review Board. Human SAT was obtained from discarded tissue of five patients undergoing panniculectromy at UMass Memorial Hospital. Adipose tissue SVF cells were prepared from collagenase-digested adipose tissue. In brief, fat pads were digested with 2 mg/ml collagenase (Sigma-Aldrich) at 37°C for 45 min, filtered through 100 μm BD Falcon cell strainers, and spun at 300 × *g* for 10 min at room temperature. The adipocyte layer and the supernatant were aspirated, and the pelleted cells were collected as the SVF.

Liver and Spleen Cell Isolation

Liver cells were isolated as previously described (Page and Garvey, 1979). Spleens were manually dissociated, and the resultant cell suspension was centrifuged at 500 × *g*.

Flow Cytometry

For mice, cells were resuspended in PBS containing 1% BSA (fluorescence-activated cell sorting buffer) and Fc Block (eBioscience) and allowed to block nonspecific binding for 15 min at 4°C. Then, cells were counted and incubated for an additional 20 min in the dark at 4°C with fluorophore-conjugated primary antibodies or isotype control antibodies. See the Supplemental Experimental Procedures for a complete list of the antibodies used.

For the EdU experiments, cells were surface stained according to manufacturer's instructions. After incubation with primary antibodies, cells were washed and fixed with Fixation/Permeabilization Concentrate buffer (eBioscience) and then permeabilized with permeabilization buffer (eBioscience). EdU was chemically conjugated to Alexa 405 or Alexa 647 fluorophore according to the instructions of the manufacturer (Invitrogen). Sample data were acquired on a BD LSRII flow cytometer (BD Biosciences) and analyzed with FlowJo (Tree Star).

Liposome Preparation and Depletion of Blood Monocytes

PBS and clodronate-loaded liposomes were prepared in a precisely scaled-down version of a method previously described (van Rooijen and van Kesteren-Hendrikx, 2003). *ob/ob* mice were i.v. injected with 200 μl of clodronate-loaded liposomes or an equal volume of PBS-loaded liposomes every 16 hr. Small amounts of blood were taken at the end of several of the 16 hr periods and immediately before subsequent liposome injection in order to ensure that monocyte depletion was continuous. Untreated mice did not receive any injections. The mice were given drinking water containing 1 mg/ml EdU 18 hr after the initial liposome injection. ATM content and EdU incorporation into ATMs were assessed by flow cytometric analysis 32 and 80 hr after exposure to EdU drinking water.

Explants and Treatments

Pieces (1–2 mm^3) of VAT from *ob/ob* mice were treated with 10 μM EdU and 1 or 10 ng/ml of MCP-1 (Invitrogen). After 48 hr of treatment, SVF cells were isolated, counted, and analyzed by flow cytometry.

Immunohistochemistry

Adipose tissue SVF cells and sections were stained and analyzed by fluorescent microscopy as previously described (Aouadi et al., 2013).

Isolation of RNA and Real Time PCR

RNA isolation was performed according to the Trizol Reagent Protocol (Invitrogen). cDNA was synthesized from 0.5–1 μg of total RNA with an iScript cDNA Synthesis Kit (Bio-Rad) according to the manufacturer's instructions. For real-time PCR, synthesized cDNA forward and reverse primers along with the iQ SYBR Green Supermix were run on the CFX96 Touch Real-Time PCR Detection System (Bio-Rad). The ribosomal mRNA 36B4 was used as an internal loading control.

Figure 4. MCP-1 Is Required for Optimal Adipose Tissue Macrophage Proliferation

(A–D) *il4* (A), *mcsf* (B), *opn* (C), and *mcp-1* (D) expression was measured by RT-PCR. n = 5.

(E and F) Expression of *opn* (E) and *mcp-1* (F) in SAT, VAT, and liver from mice fed an ND or HFD for 7 weeks. n = 5.

(G) Expression of *mcp-1* in VAT of mice fed an HFD for 7 weeks and fasted for 24 hr.

(H and I) Percentage (H) and number (I) of macrophages in SVF from VAT of MCP-1 KO and WT mice fed an HFD for 6 weeks and fasted for 18 hr. n = 5.

(J and K) Percentage (J) and number (K) of EdU$^+$ macrophages in AT of MCP-1 KO and WT mice.

(L–N) Number of blood monocytes in MCP-1 KO and WT mice (L). Explants from VAT of five *ob/ob* mice were treated with 1 and 10 ng/ml of MCP-1 in presence of 10 μM of EdU for 48 hr. Graph represents the number of macrophages (M) and EdU$^+$ (N) macrophages in explants.

(O) Body weight of MCP-1 KO and WT mice fed an HFD for 6 weeks.

(P and Q) GTT (P) and fasting glycaemia (Q). All graphs are expressed as mean ± SEM. Statistical significance was determined by a Student's t test or two-way ANOVA followed by a Tukey post hoc test. ***p < 0.001; **p < 0.01; *p < 0.05.

VAT was isolated from mice fed am ND or HFD for 7 weeks. See also Figure S4.

Statistical Analysis

All values are shown as means ± SEM. A Student's t test for two-tailed distributions with equal variances was used for comparison between two groups. $p \leq 0.05$ was considered significant. Statistical analyses were performed with GraphPad Prism 5.

Please see the Supplemental Information for detailed experimental procedures and additional data.

SUPPLEMENTAL INFORMATION

Supplemental Information contains Supplemental Experimental Procedures and four figures and can be found with this article online at http://dx.doi.org/10.1016/j.cmet.2013.11.017.

ACKNOWLEDGMENTS

We thank Drs. S. Corvera, H. Kornfeld, S. Levitz, D. Greiner, J. Harris, and J. Virbasius and members of our laboratory group for excellent discussion of the data in this paper. We also appreciate the help of R. Konz and the staff of Flow Cytometry and Morphology Cores in the University of Massachusetts. These studies were supported by grants to M.P.C. from the NIH (DK085753 and AI046629), a grant from the International Research Alliance at Novo Nordisk Foundation Center for Metabolic Research, a grant from the JDRF (17-2009-546), and the Core Facilities in the University of Massachusetts Diabetes and Endocrinology Research Center also funded by the NIH (DK325220). J.L.C. is supported by the NIDDK of the NIH under NRSA postdoctoral fellowship F32DK098879.

Received: August 22, 2012
Revised: June 4, 2013
Accepted: November 15, 2013
Published: December 26, 2013

REFERENCES

Allavena, P., Bianchi, G., Zhou, D., van Damme, J., Jílek, P., Sozzani, S., and Mantovani, A. (1994). Induction of natural killer cell migration by monocyte chemotactic protein-1, -2 and -3. Eur. J. Immunol. *24*, 3233–3236.

Aouadi, M., Tencerova, M., Vangala, P., Yawe, J.C., Nicoloro, S.M., Amano, S.U., Cohen, J.L., and Czech, M.P. (2013). Gene silencing in adipose tissue macrophages regulates whole-body metabolism in obese mice. Proc. Natl. Acad. Sci. USA *110*, 8278–8283.

Asterholm, I.W., McDonald, J., Blanchard, P.G., Sinha, M., Xiao, Q., Mistry, J., Rutkowski, J.M., Deshaies, Y., Brekken, R.A., and Scherer, P.E. (2012). Lack of "immunological fitness" during fasting in metabolically challenged animals. J. Lipid Res. *53*, 1254–1267.

Bjornson, B.H., Harvey, J.M., and Rose, L. (1985). Differential effect of hydrocortisone on eosinophil and neutrophil proliferation. J. Clin. Invest. *76*, 924–929.

Bourlier, V., Zakaroff-Girard, A., Miranville, A., De Barros, S., Maumus, M., Sengenes, C., Galitzky, J., Lafontan, M., Karpe, F., Frayn, K.N., and Bouloumié, A. (2008). Remodeling phenotype of human subcutaneous adipose tissue macrophages. Circulation *117*, 806–815.

Feng, B., Jiao, P., Nie, Y., Kim, T., Jun, D., van Rooijen, N., Yang, Z., and Xu, H. (2011). Clodronate liposomes improve metabolic profile and reduce visceral adipose macrophage content in diet-induced obese mice. PLoS ONE *6*, e24358.

Guilherme, A., Virbasius, J.V., Puri, V., and Czech, M.P. (2008). Adipocyte dysfunctions linking obesity to insulin resistance and type 2 diabetes. Nat. Rev. Mol. Cell Biol. *9*, 367–377.

Hashimoto, D., Chow, A., Noizat, C., Teo, P., Beasley, M.B., Leboeuf, M., Becker, C.D., See, P., Price, J., Lucas, D., et al. (2013). Tissue-resident macrophages self-maintain locally throughout adult life with minimal contribution from circulating monocytes. Immunity *38*, 792–804.

Hinojosa, A.E., Garcia-Bueno, B., Leza, J.C., and Madrigal, J.L. (2011). CCL2/MCP-1 modulation of microglial activation and proliferation. J. Neuroinflammation *8*, 77.

Inouye, K.E., Shi, H., Howard, J.K., Daly, C.H., Lord, G.M., Rollins, B.J., and Flier, J.S. (2007). Absence of CC chemokine ligand 2 does not limit obesity-associated infiltration of macrophages into adipose tissue. Diabetes *56*, 2242–2250.

Jenkins, S.J., Ruckerl, D., Cook, P.C., Jones, L.H., Finkelman, F.D., van Rooijen, N., MacDonald, A.S., and Allen, J.E. (2011). Local macrophage proliferation, rather than recruitment from the blood, is a signature of TH2 inflammation. Science *332*, 1284–1288.

Jimenez, F., Quinones, M.P., Martinez, H.G., Estrada, C.A., Clark, K., Garavito, E., Ibarra, J., Melby, P.C., and Ahuja, S.S. (2010). CCR2 plays a critical role in dendritic cell maturation: possible role of CCL2 and NF-kappa B. J. Immunol. *184*, 5571–5581.

Kanda, H., Tateya, S., Tamori, Y., Kotani, K., Hiasa, K., Kitazawa, R., Kitazawa, S., Miyachi, H., Maeda, S., Egashira, K., and Kasuga, M. (2006). MCP-1 contributes to macrophage infiltration into adipose tissue, insulin resistance, and hepatic steatosis in obesity. J. Clin. Invest. *116*, 1494–1505.

Kosteli, A., Sugaru, E., Haemmerle, G., Martin, J.F., Lei, J., Zechner, R., and Ferrante, A.W., Jr. (2010). Weight loss and lipolysis promote a dynamic immune response in murine adipose tissue. J. Clin. Invest. *120*, 3466–3479.

Lee, Y.H., Petkova, A.P., Mottillo, E.P., and Granneman, J.G. (2012). In vivo identification of bipotential adipocyte progenitors recruited by β3-adrenoceptor activation and high-fat feeding. Cell Metab. *15*, 480–491.

Lumeng, C.N., DelProposto, J.B., Westcott, D.J., and Saltiel, A.R. (2008). Phenotypic switching of adipose tissue macrophages with obesity is generated by spatiotemporal differences in macrophage subtypes. Diabetes *57*, 3239–3246.

Mayi, T.H., Daoudi, M., Derudas, B., Gross, B., Bories, G., Wouters, K., Brozek, J., Caiazzo, R., Raverdi, V., Pigeyre, M., et al. (2012). Human adipose tissue macrophages display activation of cancer-related pathways. J. Biol. Chem. *287*, 21904–21913.

Morris, D.L., Cho, K.W., Delproposto, J.L., Oatmen, K.E., Geletka, L.M., Martinez-Santibanez, G., Singer, K., and Lumeng, C.N. (2013a). Adipose tissue macrophages function as antigen-presenting cells and regulate adipose tissue CD4+ T cells in mice. Diabetes *62*, 2762–2772.

Morris, D.L., Cho, K.W., Delproposto, J.L., Oatmen, K.E., Geletka, L.M., Martinez-Santibanez, G., Singer, K., and Lumeng, C.N. (2013b). Adipose tissue macrophages function as antigen-presenting cells and regulate adipose tissue CD4+ T cells in mice. Diabetes *62*, 2762–2772.

Murano, I., Barbatelli, G., Parisani, V., Latini, C., Muzzonigro, G., Castellucci, M., and Cinti, S. (2008). Dead adipocytes, detected as crown-like structures, are prevalent in visceral fat depots of genetically obese mice. J. Lipid Res. *49*, 1562–1568.

Nomiyama, T., Perez-Tilve, D., Ogawa, D., Gizard, F., Zhao, Y., Heywood, E.B., Jones, K.L., Kawamori, R., Cassis, L.A., Tschöp, M.H., and Bruemmer, D. (2007). Osteopontin mediates obesity-induced adipose tissue macrophage infiltration and insulin resistance in mice. J. Clin. Invest. *117*, 2877–2888.

Oh, D.Y., Morinaga, H., Talukdar, S., Bae, E.J., and Olefsky, J.M. (2012). Increased macrophage migration into adipose tissue in obese mice. Diabetes *61*, 346–354.

Olefsky, J.M., and Glass, C.K. (2010). Macrophages, inflammation, and insulin resistance. Annu. Rev. Physiol. *72*, 219–246.

Page, D.T., and Garvey, J.S. (1979). Isolation and characterization of hepatocytes and Kupffer cells. J. Immunol. Methods *27*, 159–173.

Sager, H.B., Middendorff, R., Rauche, K., Weil, J., Lieb, W., Schunkert, H., and Ito, W.D. (2010). Temporal patterns of blood flow and nitric oxide synthase expression affect macrophage accumulation and proliferation during collateral growth. J Angiogenes Res *2*, 18.

Scholzen, T., and Gerdes, J. (2000). The Ki-67 protein: from the known and the unknown. J. Cell. Physiol. *182*, 311–322.

Talukdar, S., Oh, Y., Bandyopadhyay, G., Li, D., Xu, J., McNelis, J., Lu, M., Li, P., Yan, Q., Zhu, Y., et al. (2012). Neutrophils mediate insulin resistance in mice fed a high-fat diet through secreted elastase. Nat. Med. *18*, 1407–1412.

van Rooijen, N., and van Kesteren-Hendrikx, E. (2003). "In vivo" depletion of macrophages by liposome-mediated "suicide". Methods Enzymol. *373*, 3–16.

Weisberg, S.P., McCann, D., Desai, M., Rosenbaum, M., Leibel, R.L., and Ferrante, A.W., Jr. (2003). Obesity is associated with macrophage accumulation in adipose tissue. J. Clin. Invest. *112*, 1796–1808.

Weisberg, S.P., Hunter, D., Huber, R., Lemieux, J., Slaymaker, S., Vaddi, K., Charo, I., Leibel, R.L., and Ferrante, A.W., Jr. (2006). CCR2 modulates inflammatory and metabolic effects of high-fat feeding. J. Clin. Invest. *116*, 115–124.

Wu, D., Molofsky, A.B., Liang, H.E., Ricardo-Gonzalez, R.R., Jouihan, H.A., Bando, J.K., Chawla, A., and Locksley, R.M. (2011). Eosinophils sustain adipose alternatively activated macrophages associated with glucose homeostasis. Science *332*, 243–247.

Xu, H., Barnes, G.T., Yang, Q., Tan, G., Yang, D., Chou, C.J., Sole, J., Nichols, A., Ross, J.S., Tartaglia, L.A., and Chen, H. (2003). Chronic inflammation in fat plays a crucial role in the development of obesity-related insulin resistance. J. Clin. Invest. *112*, 1821–1830.

Yang, J.P., and Renzi, P.M. (1993). Interleukin-2 and lymphocyte-induced eosinophil proliferation and survival in asthmatic patients. J. Allergy Clin. Immunol. *91*, 792–801.